Sound velocities and elastic properties of ??–Mg2SiO4 to 873 K by Brillouin spectroscopy

3 authors, including:

Stanislav V Sinogeikin
Carnegie Institution for Science
220 PUBLICATIONS **5,302** CITATIONS

Jay Bass
University of Illinois, Urbana-Champaign
232 PUBLICATIONS **7,735** CITATIONS

Some of the authors of this publication are also working on these related projects:

Vitreous Boron Oxide Under High Pressure View project

Elastic Constant Measurements View project

Sound velocities and elastic properties of γ-Mg₂SiO₄ to 873 K by Brillouin spectroscopy

JENNIFER M. JACKSON,* STANISLAV V. SINOGEIKIN, AND JAY D. BASS

Department of Geology, University of Illinois, Urbana, Illinois 61801, U.S.A.

ABSTRACT

The sound velocities and single-crystal elastic moduli of spinel-structured γ-Mg₂SiO₄ were measured to 873 K by Brillouin spectroscopy using a new high-temperature cell designed for single-crystal measurements. These are the first reported acoustic measurements of γ-Mg₂SiO₄ elasticity at high temperatures. A linear decrease of elastic moduli and sound velocities with temperature adequately describes the data. The adiabatic bulk modulus, K_S, shear modulus, μ, and respective temperature derivatives for γ-Mg₂SiO₄ are: $K_S = 185(3)$ GPa, $\mu = 120.4(2.0)$ GPa, $(\partial K_S/\partial T)_P = -0.024(3)$ GPa/K and $(\partial \mu/\partial T)_P = -0.015(2)$ GPa/K. Extrapolation of our data to transition zone pressures and temperatures indicates that the shear and compressional impedance contrasts associated with β- → γ-(Mg,Fe)₂SiO₄ transition are sufficient to produce an observable discontinuity at 520 km depth, even with a moderate (30–50%) amount of olivine.

INTRODUCTION

Olivine [α-(Mg,Fe)₂SiO₄] and its high-pressure polymorphs (modified spinel structured β-phase, and spinel structured γ-phase) are widely acknowledged to be major constituents of the upper mantle of the Earth. There is not, however, agreement on the question of whether the mantle is chemically layered or of uniform composition and, in particular, whether the olivine content of the mantle is constant with depth (Ringwood 1975; Bass and Anderson 1984; Weidner 1985; Anderson and Bass 1986; Duffy and Anderson 1989; Ita and Stixrude 1993; Duffy et al. 1995; Li et al. 1998; Zha et al. 1998). Numerous studies of the phase relations in (Mg,Fe)₂SiO₄ show that at mantle temperatures, the α → β and β → γ transformations in (Mg₀.₉Fe₀.₁)₂SiO₄ are relatively sharp, and occur at ~13 and 19 GPa, respectively (e.g., Katsura and Ito 1989). At 23 GPa γ-phase disproportionates into a mixture of (Mg,Fe)SiO₃ with the perovskite structure and (Mg,Fe)O (Ito and Takahashi 1989). The transition pressures roughly correspond to the pressures at seismologically determined velocity/density discontinuities at 410, 520, and 660 km (Dziewonski and Anderson 1981; Benz and Vidale 1993; Flanagan and Shearer 1998; Gaherty et al. 1999). Thus, these polymorphic phase transitions are viewed as being associated with seismic mantle discontinuities. Under this assumption, the magnitudes of observed velocity increases could be used to constrain the olivine content of the mantle, provided that laboratory elasticity data on the relevant phases are available.

Here we present single-crystal measurements on the sound velocities and elastic properties of γ-Mg₂SiO₄ at high temperatures to 873 K. To our knowledge, no other high-temperature single crystal acoustic measurements have previously been reported for this phase. Our measurements are highly complimentary to *PVT* equation of state measurements (Meng et al. 1993, 1994) and have the advantage that they provide information on the shear modulus and single-crystal stiffness constants for the material. The results are used to investigate the implications of the seismic velocity increase centered at 520 km for the olivine content of the transition zone (at depths between 410 and 660 km).

EXPERIMENTAL METHODS

For high-temperature Brillouin scattering experiments, we used a compact ceramic high-temperature (HiT) cell (Fig. 1) (Sinogeikin et al. 2000). The cell is similar in geometry and design to a Merrill-Bassett diamond anvil clamp (DAC) (Merrill and Bassett 1974) with external heating (Hazen and Finger 1981), except that the cell is designed for use at high temperature only. No pressure is generated inside the cell. The cell consists of a ceramic base, Pt-30Rh double-coil heater, and fused-silica windows with two attached thermocouples. The thermal conductivities of the ceramic parts are low, thus helping us to minimize thermal gradients in our cell. Due to the geometry of the cell, the temperature gradients are not radially symmetric throughout the cell. Our experiments show that the thermal gradients increase with increasing temperature, and that the maximum gradient measured was less than 0.01 K/μm at the highest temperature of 873 K achieved in the present study. This implies a maximum temperature difference across the sample of <1.5°. In our experiments on γ-phase, the sample was embedded in Pt foil, which should significantly lower temperature gradients from this maximum value (see below). Further details on cell design are given elsewhere (Sinogeikin et al. 2000).

The major advantage of the cell is that it is compact and can be placed onto a standard three or four-circle goniometer for measurements on single crystals. This allows the orientation

Current address: Department of Civil Engineering and Geological Sciences, University of Notre Dame, Notre Dame, IN 46556, U.S.A. E-mail: jjackson@nd.edu
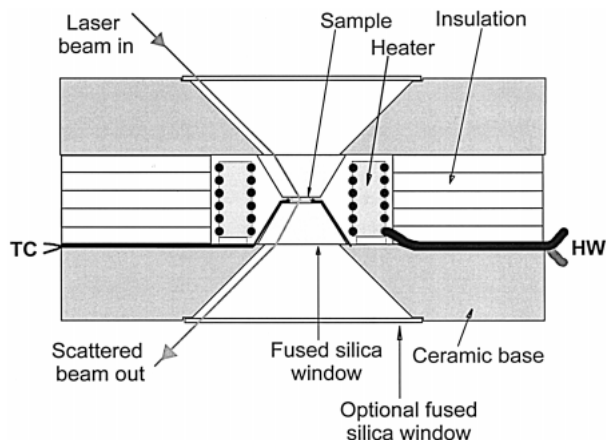
FIGURE 1. Schematic view of the ceramic high-temperature cell. TC = thermocouples, HW = heating wires.

of the sample to be varied over a broad angular range, as required for single-crystal elasticity measurements or, for example, X-ray diffraction measurements. All Brillouin measurements are performed in a symmetric/platelet (Whitfield et al. 1976) scattering geometry, in which the velocity is independent of the refractive index (RI) of the sample. This is an important consideration, because the RI can change significantly with temperature. With the HiT cell mounted on the three-circle goniometer normally used in our Brillouin experiments (Bass 1989; Sinogeikin et al. 1998a), we have excellent control over the scattering geometry, and any phonon direction within a sample plane is easily sampled by changing the χ setting on the goniometer. For symmetries higher than monoclinic the HiT cell allows determination of the complete elasticity tensor as a function of temperature from a single sample with the dimensions of about 100 μm × 100 μm × 20 μm or even smaller. The small samples used with our cell distinguish this experiment from other high temperature ultrasonic (Sumino et al. 1983; Isaak et al. 1989) and Brillouin (Zouboulis and Grimsditch 1991) studies on minerals.

The single-crystal samples of γ-Mg_2SiO_4 spinel were approximately 100–150 μm in size and were synthesized at the Center for High Pressure Research at Stony Brook. X-ray diffraction studies were performed to verify the samples were indeed γ-Mg_2SiO_4 spinel [a = 8.0687(7) Å]. The samples were colorless and optically isotropic in visible light.

The room-temperature elastic properties of γ-Mg_2SiO_4 were initially determined by Weidner et al. (1984). This phase is cubic, and its elasticity is therefore completely characterized by three independent elastic moduli, namely C_{11}, C_{44}, and C_{12}. All of these constants can be obtained by measuring the acoustic velocities in a few non-equivalent crystallographic directions in a single crystallographic plane.

Because the crystals were extremely small, it was difficult to attach them directly to the silica windows using a ceramic adhesive. To overcome this problem we placed the samples into 150 μm diameter holes made in 1 mm × 3 mm × 0.25 mm thick platinum foil strips. The empty spaces in the holes were filled with high-temperature alumina cement. After the adhe-

sive dried, we polished both sides of the foil until a final thickness of 20 μm was achieved. Thus, we obtained samples with two flat nearly parallel surfaces, surrounded by platinum foil and suitable for Brillouin scattering in platelet/symmetric geometry. The unit vector normal to the polished surfaces of the sample has direction cosines of approximately (0.040, 0.077, 0.333). The foil with the embedded sample was glued to the fused silica window with high-temperature adhesive (Fig. 2). Optical observations showed that there was no direct contact between the sample and the window. No reaction of the adhesive with the samples was observed at high temperature.

The heater was powered with a digital DC power supply, which allowed us to set the experimental temperature to within 0.5° of the target temperature. The power during the experiment was set and adjusted manually. The temperature was measured with two type K (Chromel-Alumel) thermocouples placed on opposite sides of the sample (Fig. 2). The thermocouple readings were recorded with a computer acquisition board.

At each temperature, a set of measurements consisted of several runs, each with the sample in a different orientation to probe different phonon directions. During an individual run, the temperature usually fluctuated by less than 1 degree, and the maximum variation was less than 2°. Each run lasted between 10–20
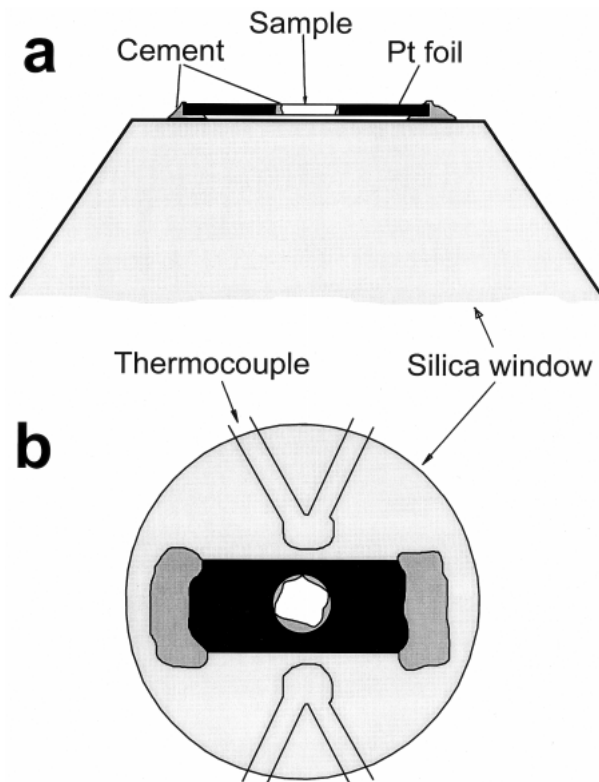
FIGURE 2. Side (**a**) and top (**b**) view of the sample attachment to the window. The thermocouples shown are attached to the opposite window.

minutes. The temperature of the sample was taken to be the average of the two thermocouple readings, which differed by less than 3° at the highest temperature. Calibration runs with a thermocouple at the sample position confirms the validity of this approach. We note that the presence of Pt foil as a sample holder helps to eliminate thermal gradients near the sample.

All Brillouin experiments were performed in an 80° platelet/symmetric scattering geometry. We used an Argon ion laser (λ = 5145 Å) and a piezoelectrically scanned 6-pass tandem Fabry-Perot interferometer. A detailed description of the Brillouin setup is given by Sinogeikin et al. (1998a).

RESULTS

All Brillouin spectra were of excellent quality, with a high signal-to-noise ratio. Figure 3 shows representative spectrum. In most of the spectra one or both Brillouin peaks from fused silica were observed and used as a cross-check that there are no significant deviations from symmetric scattering geometry and the proper scattering angle. Brillouin data were collected at five temperatures: 298, 478, 623, 773, and 873 K. At 298 and 773 K the spectra were collected in 13 crystallographic directions spaced at 15° in the sample plane (Fig. 4). At 478 and 623 K the data were collected in seven crystallographic directions with an angular increment of 30°. At 873 K the data were collected in eight directions with an angular increment of 15°. The quality of the spectra improved with increasing temperature until it was heated for several hours at 873 K. During the experiment at 873 K the sample started to crack, which made the sample unsuitable for further experiments. Optical observations with a polarizing microscope indicated that the sample had fractured into 10–20 μm blocks, all of which remained transparent and optically isotropic. This is consistent with the observations of Suzuki et al. (1979), who performed measurements on the thermal expansion of γ-Mg_2SiO_4 to 1023 K by powder X-ray diffraction.
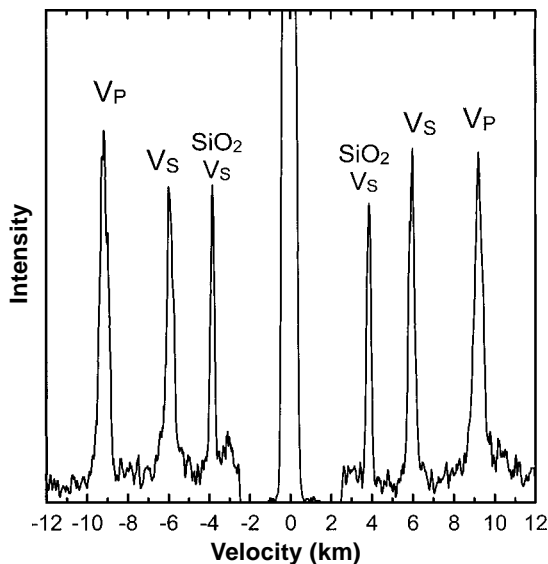
The λ-phase is elastically anisotropic with an anisotropy factor [defined as $A = (2C_{44} + C_{12})/C_{11} - 1$ (Karki et al. 1997)] at room temperature of $A = 0.15$. This anisotropy makes it possible to obtain a least-squares solution for both the single-crystal elastic moduli and the phonon directions within a known crystallographic plane from the 26 acoustic mode velocities collected at room temperature. The error in phonon direction determination by this method is estimated to be about 2°. We used the same procedure with the data collected at 773 K, and the results of these two phonon direction determinations are in mutual agreement.

The calculated phonon directions were used as input to a linearized inversion procedure (Weidner and Carleton 1977) to solve for the 3 independent elastic moduli at each temperature (Table 1). The 2° uncertainties in the phonon direction were accounted for when calculating the uncertainties in the C_{ij} values from the inversion. For the purposes of the inversion, we used the thermal expansion data of Suzuki et al. (1979) to calculate the density at each experimental temperature. The aggregate adiabatic bulk modulus, shear modulus, and aggregate acoustic velocities were calculated from the C_{ij} values using the Voigt-Reuss-Hill (VRH) averaging scheme (Table 1, Figs. 5–7). The room-temperature elastic moduli and aggregate acoustic velocities are in agreement with earlier measurements by Weidner et al. (1984).
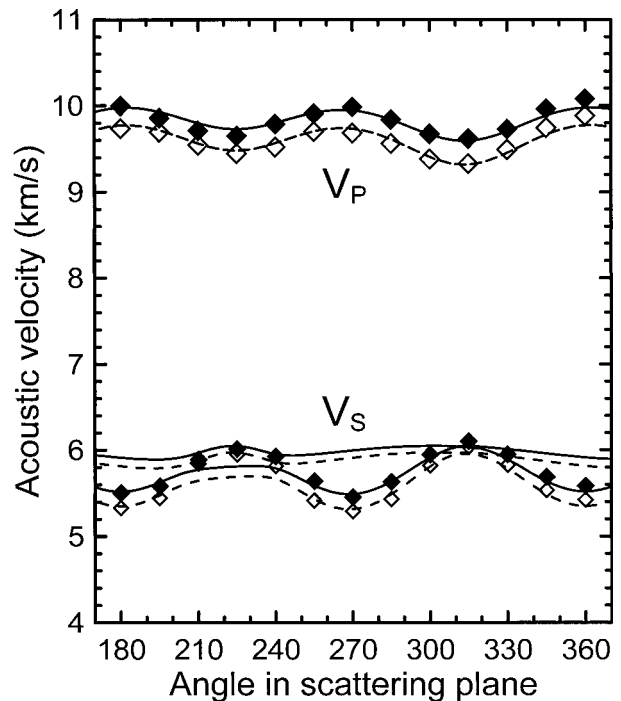
FIGURE 4. Measured acoustic velocities as a function of angle in the scattering plane at 298 K (solid symbols) and 773 K (open symbols). The lines show acoustic velocities calculated from the best fit single-crystal elastic moduli (solid line for 298 K and dashed line for 773 K).

FIGURE 3. Brillouin spectrum of γ-Mg_2SiO_4 collected at 873 K.

TABLE 1. Single-crystal elastic moduli, aggregate elastic moduli and acoustic velocities in γ-Mg_2SiO_4 as a function of temperature measured in this experiment

Temperature (K)	Density (g/cm³)	C_{11} (GPa)	C_{44} (GPa)	C_{12} (GPa)	K_S (GPa)	μ (GPa)	V_P (km/s)	V_S (km/s)	A
298	3.559	327(3)	131(2)	114(2)	185 (3)	120 (2)	9.85 (6)	5.82 (3)	0.148
478	3.546	319(3)	128(2)	114(2)	183 (3)	117 (2)	9.78 (7)	5.75 (4)	0.159
623	3.532	313(3)	129(2)	110(2)	177 (3)	117 (2)	9.72 (7)	5.76 (4)	0.172
773	3.519	305(3)	125(2)	108(2)	174 (3)	114 (2)	9.62 (7)	5.69 (4)	0.177
873	3.509	295(4)	123(2)	108(3)	170 (3)	110 (2)	9.51 (8)	5.61 (5)	0.200

Notes: Aggregate elastic moduli and acoustic velocities are calculated using Voigt-Reuss-Hill averaging scheme. The anisotropy factor is calculated as $A = (2C_{44} + C_{12})/C_{11} - 1$ (Karki et al. 1997).
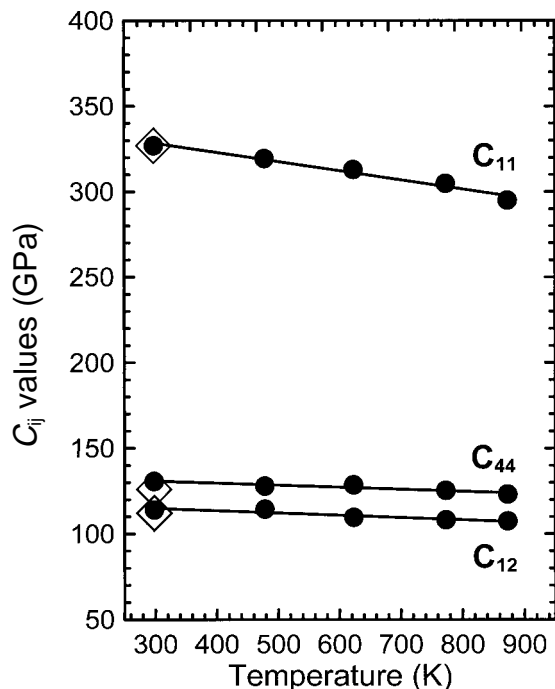
FIGURE 5. Single crystal elastic moduli of γ-Mg_2SiO_4 as a function of temperature. Circles = this study; diamonds = Weidner et al. (1984).
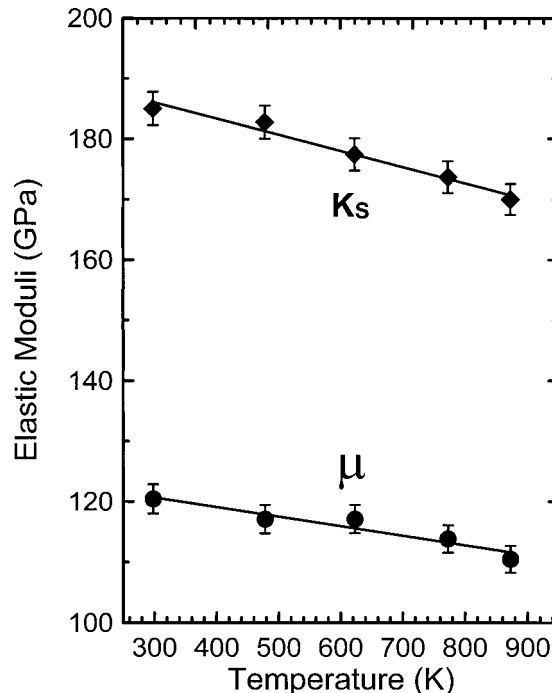
FIGURE 6. Aggregate elastic moduli of γ-Mg_2SiO_4 as a function of temperature.

Within the uncertainties all elastic moduli exhibit a linear dependence on temperature over the temperature range of our experiments, yielding the temperature derivatives for γ-Mg_2SiO_4 as listed in Table 2. The only published numbers with which our results can be compared are those by Meng et al. (1993, 1994). These authors measured the isothermal compressibility of γ-phase by synchrotron X-ray diffraction measurements at high temperatures and pressures using both a cubic anvil apparatus (Meng et al. 1993) and an externally heated diamond anvil cell (Meng et al. 1994). They obtained mutually consistent results for the temperature derivative of the isothermal bulk modulus in the range of –0.027 to –0.028 GPa/K, from which they calculated the temperature derivative of the adiabatic bulk modulus to be –0.020 GPa/K. Our value of $(\partial K_S/\partial T)_P = -0.024(3)$ is in agreement with the results of Meng and co-workers.

Within the uncertainties of the experiment our aggregate acoustic velocities can also be described by linear functions: $V_P = 10.01 - 5.34 \cdot 10^{-4} \cdot (T - 298)$ and $V_S = 5.91 - 3.07 \cdot 10^{-4} \cdot (T - 298)$ km/s (T is in Kelvin) over the experimental temperature range. This implies that both V_P and V_S decrease by ~0.5(1)% per 100 K.

Seismological studies suggest that there is no measurable velocity anisotropy in the transition zone (Gaherty et al. 1999) within the field of stability of γ-phase. This is consistent with the fact that γ-Mg_2SiO_4 exhibits only moderate elastic anisotropy at room temperature. It is interesting to note that the anisotropy of the spinel phase increases with increasing temperature, as it does for MgO (Chen et al. 1998). The anisotropy factor for γ-phase increases linearly from 0.15 at room temperature to 0.20 at 873 K. On the other hand, the elastic anisotropy of γ-
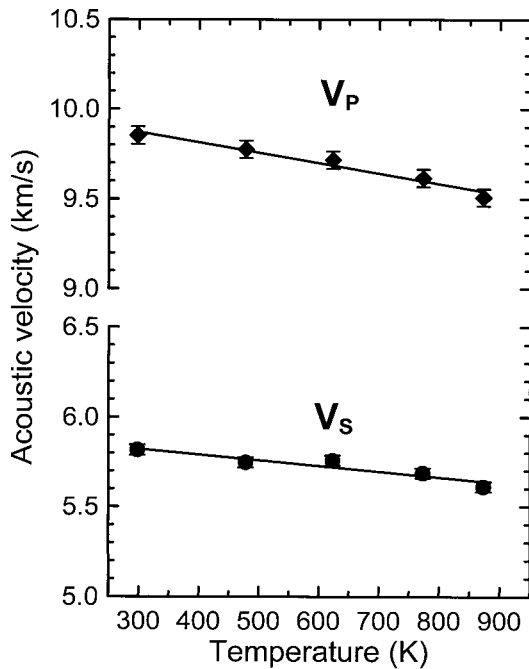
FIGURE 7. Aggregate compressional and shear velocities of γ-Mg_2SiO_4 as a function of temperature.

TABLE 2. Single crystal elastic moduli, aggregate moduli (GPa) and respective temperature derivatives (GPa/K) for γ-Mg_2SiO_4

	This Study	Weidner et al. 1984	Meng et al. 1993
C_{11}	327 (3)	327(4)	
$(\partial C_{11}/\partial T)_P$	−0.050 (4)		
C_{44}	130.7 (3.0)	126 (2)	
$(\partial C_{44}/\partial T)_P$	−0.012 (3)		
C_{12}	114 (2)	112 (3)	
$(\partial C_{12}/\partial T)_P$	−0.011 (3)		
K_S	185 (3)	184	184
$(\partial K_S/\partial T)_P$	−0.024 (3)		−0.020
μ	120.4 (2.0)	119	
$(\partial \mu/\partial T)_P$	−0.015 (2)		

Note: Calculated from K_T = 182.6 GPa and α of Meng et al. (1993) and γ_{th} of Watanabe (1987).

gested that the 520 km discontinuity may not be sharp [e.g., less than 10 km (Benz and Vidale 1993)], but is perhaps a rather broad (25–50 km) velocity gradient (Revenaugh and Jordan 1991). The width of this feature is consistent with the width of $\beta \rightarrow \gamma$ transition, which reaches 25 km for an Fe content of 10% (Katsura and Ito 1989). Although there is evidence suggesting that this discontinuity is a global feature (Flanagan and Shearer 1998), the lack of routine observations of a 520 km discontinuity in refraction studies suggests that the bulk of the impedance change may occur in density rather than velocity (Shearer 1996). Table 3 lists the velocity and impedance contrasts from several different seismic studies in which the 520 km discontinuity was observed. A significant degree of scatter exists in the estimates of both velocity and impedance contrast, and the variation in values for longitudinal and shear waves are not well correlated. Whereas global observations suggest approximately equal impedance contrasts for both V_P and V_S (Shearer 1990, 1991), more recent regional models imply a smaller contrast for V_P than for V_S (Gaherty et al. 1996, 1999; Kato and Jordan 1999).

The first measurements of the elastic properties of β- and γ-Mg_2SiO_4 at ambient conditions (Sawamoto et al. 1984; Weidner et al. 1984) found the elastic properties of β- and γ-phases to be very similar, which implies that this transformation is not likely to be associated with a seismic discontinuity. Subsequent measurements of the acoustic velocities in γ-Mg_2SiO_4 by ultrasonic interferometry to 3 GPa at room temperature (Rigden et al. 1991, 1992) reinforced this conclusion. Rigden et al. (1991, 1992) further suggested that although the impedance contrast of the $\beta \rightarrow \gamma$ transformation might be observable in seismic reflection studies, an olivine content well in excess of 50% would be required. However, these studies did not take into account the variations of velocities and density with Fe content for the β- and γ-phases. Sinogeikin et al. (1997, 1998a) measured the dependence of the elastic properties and acoustic velocities on Fe content for β- and γ-$(Mg,Fe)_2SiO_4$, and found that at room pressure and temperature, both the velocity and impedance contrasts for the $\beta \rightarrow \gamma$ transition increase with increasing Fe content.

The measurements of this study along with extant results on the high-temperature and high-pressure elasticity of β- and γ-phases, allow us to extrapolate the elastic moduli and acous-

phase decreases by a factor of four with increasing pressure from room-pressure to 16 GPa (Sinogeikin et al. 1998b). From these results we infer that at transition zone conditions γ-phase will be slightly anisotropic, but not to a degree which induces significant seismic anisotropy in the Earth.

Implications for 520 km discontinuity

Seismic discontinuities at approximately 410, 520, and 660 km depth are often associated with the α(olivine) $\rightarrow$ β-phase, $\beta \rightarrow \gamma$, and $\gamma \rightarrow$ Perovskite + (Mg,Fe)O transformations, respectively, for olivine of approximately Fo_{90} composition. In contrast to the 410 and 660 km discontinuities, which are sharp features with reasonably well defined velocity increases of about 5% in both V_P and V_S (Dziewonski and Anderson 1981), the 520 km discontinuity is comparatively small and there is less agreement on the magnitude of the velocity jump. It has been sug-

TABLE 3. Velocity and impedance contrasts at 520 km discontinuity

Depth (km)	ΔV_P (%)	$\Delta(\rho V_P)$ (%)	ΔV_S (%)	$\Delta(\rho V_S)$ (%)	Observ.	Ref.
514-526	1.2–4.8	2.4–7.2	1.2–4.8	2.4–7.2	Global	1
519			1.44	2.2–3.6	Global	2
520				1.4–2.0	Pacific	3
520				2.0	Global	4
550	2.0–3.0				Eurasia	5
530	2.55				Eurasia	6
540	3.0				Eurasia	7
520		3.0		3.0	Global	8
507	0.7	1.5	1.5	2.3	W. Pacific	9
520	0.1	0.4	1.3	1.6	Philippine	10
499	0.3	1.1	0.8	1.5	Australia	11

Notes: Sources of data are: 1 = (Shearer 1991), 2 = (Shearer 1996), 3 = (Revenaugh and Jordan 1991), 4 = (Gossler and Kind 1996), 5 = (Mechie et al. 1993), 6 = (Ryberg et al. 1997), 7 = (Oreshin et al. 1998), 8 = (Shearer 1990), 9 = (Gaherty et al. 1996), 10 = (Kato and Jordan 1999), 11 = (Gaherty et al. 1999).

tic velocities of these phases to the *P-T* conditions of the 520 km discontinuity. We used the formalism of Duffy and Anderson (1989), to calculate acoustic velocities, elastic moduli, and density of β and γ phases of $(Mg_{0.9}Fe_{0.1})_2SiO_4$ along a 1673 K adiabat. The input parameters used for the calculations are based on the most recent experimental results on the composition, pressure, and temperature dependence of the elasticity of β- and γ-phases (Table 4). In general, we chose to use acoustically determined properties over those obtained by static compression techniques, except for the temperature derivative of the adiabatic bulk modulus of the β phase. Although the temperature derivative of the adiabatic bulk modulus for $\beta-Mg_2SiO_4$ was recently measured by Li et al. (1998) their results differ significantly from values reported in earlier study by Meng et al. (1993) and by Fei et al. (1992). These later authors measured $(\partial K_T/\partial T)_P$ of $\beta-(Mg,Fe)_2SiO_4$ by high *P-T* synchrotron X-ray diffraction experiments, and from these measurements $(\partial K_S/\partial T)_P$ can be calculated (See Jackson and Rigden 1996). Because of this uncertainty in $(\partial K_S/\partial T)_P$ for β-phase, we used both available results in our extrapolation of the velocities and density to transition zone pressures and temperatures That is, we performed calculations using both values of $(\partial K_S/\partial T)_P = -0.012$ and -0.019 GPa/K for β-phase (Table 5, Figure 8). The results of our calculations (Table 6, Fig. 8), demonstrate that the impedance contrast is fairly insensitive to the choice of the $(\partial K_S/\partial T)_P$, although the compressional velocity contrast is more strongly affected by varying $(\partial K_S/\partial T)_P$. When the values from this study and Li et al. (1998) for $(\partial K_S/\partial T)_P$ are used in calculations, the compressional velocities for β- and γ-$(Mg_{0.9}Fe_{0.1})_2SiO_4$ become undistinguishable at the *P-T* conditions of the 520 km discontinuity.

TABLE 4. Input parameters for extrapolating the elastic properties of β- and γ-$(Mg_{0.9}Fe_{0.1})_2SiO_4$ to temperature and pressure conditions of the 520 km discontinuity

	Density	K_s^*	$\partial K_s/\partial P\vert_T$	$\partial K_s/\partial T\vert_P$	μ^*	$\partial\mu/\partial P\vert_T$	$\partial\mu/\partial T\vert_P$
β	3.596	170	4.2†	−0.012‡ −0.019§	108	1.5†	−0.017‡
γ	3.687	189	4.1‖	−0.024#	118	1.3‖	−0.015#

Notes: We assume that the effect of Fe on the temperature derivatives of γ-phase is not significant.
* Sinogeikin et al. (1998a).
† Zha et al. (1998); Li et al. (1996).
‡ Li et al. (1998).
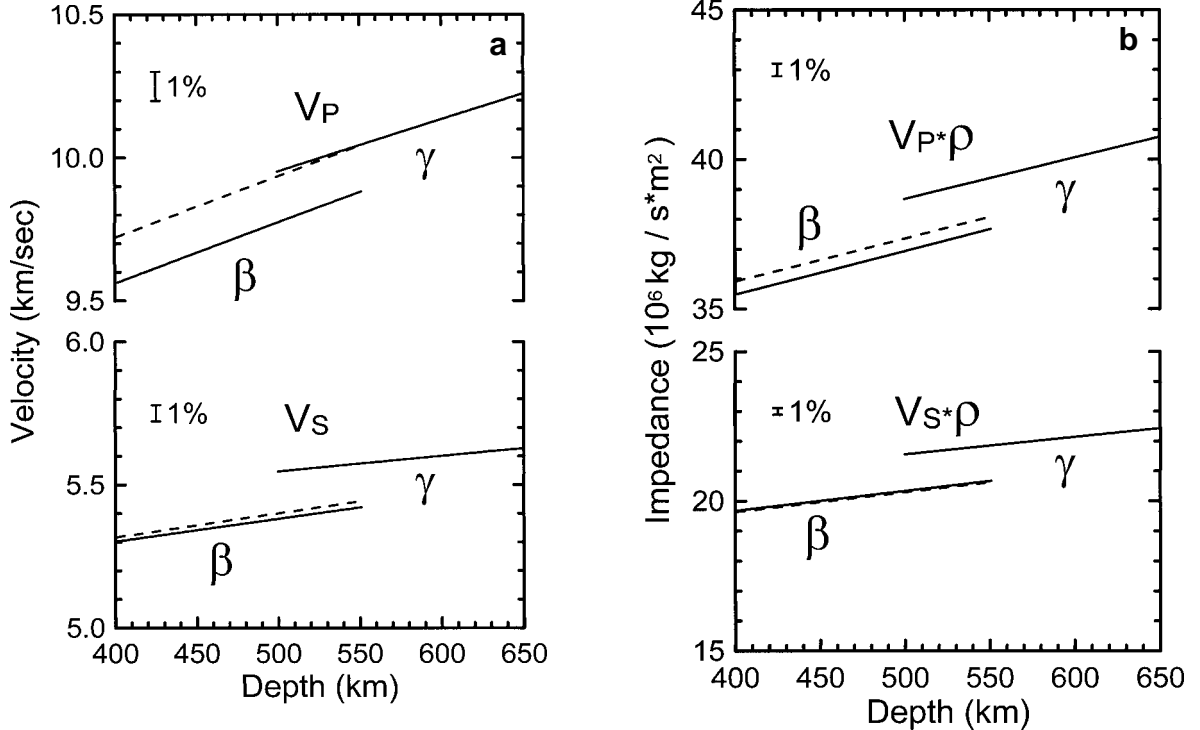§ Jackson and Rigden (1996).
‖ Sinogeikin et al. (1998b).
This study.

TABLE 5. Calculated elastic moduli and velocities of β- and γ-phases of $(Mg_{0.9}Fe_{0.1})_2SiO_4$ at the 520 km discontinuity for different input parameters

$(\partial K_s/\partial T)_P$ (GPa/K)	Density (g/cm³)	K_S (GPa)	μ (GPa)	V_P (km/s)	V_S (km/s)
β −0.012	3.773	228.1	110.71	9.980	5.417
β −0.019	3.792	218.1	110.4	9.816	5.397
γ −0.024	3.901	228.67	120.5	9.990	5.558

FIGURE 8. Acoustic velocities (**a**) and impedance (ρV) (**b**) in β- and γ-$(Mg,Fe)_2SiO_4$ with 10 mol% Fe calculated along 1673 K adiabat. Solid line for β-phase corresponds to $(\partial K_s/\partial T)_P = -0.019$ GPa/K (Jackson and Rigden 1996) and dashed line corresponds to $(\partial K_s/\partial T)_P = -0.012$ GPa/K (Li et al. 1998). The difference in the temperature derivative has a very small effect on the shear velocity and shear impedance of β-phase. Although it has a very significant effect on the longitudinal velocity, its effect on longitudinal impedance is not significant.

TABLE 6. Velocity and impedance contrasts at the 520 km discontinuity (1673 K adiabat, 18 GPa) calculated with different input parameters for β-$(Mg_{0.9}Fe_{0.1})_2SiO_4$

$(\partial K_S/\partial T)_P$ (GPa/K)	$\Delta\rho$ (%)	ΔV_P (%)	ΔV_S (%)	$\Delta(\rho V_P)$ (%)	$\Delta(\rho V_S)$ (%)
−0.012	3.3	0.1	2.6	3.4	5.9
−0.019	2.8	1.8	2.9	4.6	5.8

The impedance contrasts for the β → γ-$(Mg_{0.9}Fe_{0.1})_2SiO_4$ phase transition (Table 6) can be compared with seismological observations to constrain the proportion of olivine in the transition zone. Comparing the calculated shear impedance contrast (~6%, independent of the choice of $(\partial K_S/\partial T)_P$ for β-phase) with the seismological determinations (average of 2–3%, Table 3), we infer that an olivine content of 30–50% by volume is sufficient to account for the shear impedance contrast at the 520 km discontinuity. The values for the longitudinal impedance contrast (both calculated and observed) show far more scatter and, therefore, provide little constraint on the proportion of olivine, although they are not inconsistent with conclusions based on the shear impedance contrasts. A set of results which are difficult to explain are high (2–3%) ΔV_P contrasts reported for the sub-Eurasian mantle. Even a transition zone composed of 100% olivine cannot produce such a large V_P contrast at 520 km due to the β → γ transition alone, and the Eurasia results may require a different explanation such as regional chemical heterogeneity caused by accumulation of subducted material on top of the 660 km discontinuity.

REFERENCES CITED

Anderson, D.L. and Bass, J.D. (1986) Transition region of the Earth's upper mantle. Nature, 320, 321–328.

Bass, J.D. (1989) Elasticity of grossular and spessartite garnets by Brillouin spectroscopy. Journal of Geophysical Research, 94, 7621–7628.

Bass, J.D. and Anderson, D.L. (1984) Composition of the upper mantle: geophysical test of two petrological models. Geophysical Research Letters, 11, 237–240.

Benz, H.M. and Vidale, J.E. (1993) Sharpness of upper-mantle discontinuities determined from high-frequency reflections. Nature, 365, 147–150.

Chen, G., Liebermann, R.C., and Weidner, D.J. (1998) Elasticity of single-crystal MgO to 8 Gigapascals and 1600 Kelvin. Science, 280, 1913–1916.

Duffy, T.S. and Anderson, D.L. (1989) Seismic velocities in mantle minerals and the mineralogy of the upper mantle. Journal of Geophysical Research, 94, 1895–1912.

Duffy, T.S., Zha, C.-S., Downs, R.T., Mao, H.-K., and Hemley, R.J. (1995) Elasticity of forsterite to 16 GPa and the composition of the upper mantle. Nature, 378, 170–173.

Dziewonski, A.M. and Anderson, D.L. (1981) Preliminary reference Earth model. Physics of the Earth and Planetary Interiors, 25, 297–356.

Fei, Y., Mao, H.-K., Shu, J., Parthasarathy, G., Bassett, W.A., and Ko, J. (1992) Simultaneous high-P, high-T X-ray diffraction study of β-$(Mg,Fe)_2SiO_4$ to 26 GPa and 900 K. Journal of Geophysical Research, 97, 4489–4495.

Flanagan, M.P. and Shearer, P.M. (1998) Global mapping of topography on transition zone velocity discontinuities by stacking SS precursors. Journal of Geophysical Research, 103, 2673–2692.

Gaherty, J.B., Jordan, T.H., and Gee, L.S. (1996) Depth extent of polarization anisotropy in western Pacific upper mantle. Journal of Geophysical Research, 101, 22291–22309.

Gaherty, J.B., Kato, M., and Jordan, T.H. (1999) Seismological structure of the upper mantle: a regional comparison of seismic layering. Physics of the Earth and Planetary Interiors, 110, 21–41.

Gossler, J. and Kind, R. (1996) Seismic evidence for very deep roots of continents.

Earth and Planetary Science Letters, 138, 1–13.

Hazen, R.M. and Finger, L.W. (1981) High-temperature diamond-anvil pressure cell for single-crystal studies. Review of Scientific Instruments, 52, 75–79.

Isaak, D.G., Anderson, O.L., and Goto, T. (1989) Measured elastic moduli of single-crystal MgO up to 1800 K. Physics and Chemistry of Minerals, 16, 704–713.

Ita, J. and Stixrude, L. (1993) Density and elasticity of the model upper mantle compositions and their implications for whole structure. In E. Takahashi, R. Jeanloz, and D. Rubie, Eds., Evolution of the Earth and planets. Geophysical monograph 74, IUGG volume 14, p. 111–130. IUGG/AGU, Washington, D.C.

Ito, E. and Takahashi, E. (1989) Postspinel transformations in the system Mg_2SiO_4-Fe_2SiO_4 and some geophysical implications. Journal of Geophysical Research, 94, 10637–10646.

Jackson, I. and Rigden, S.M. (1996) Analysis of P-V-T data: constraints on the thermoelastic properties of high-pressure minerals. Physics of the Earth and Planetary Interiors, 96, 85–112.

Karki, B.B., Stixrude, L., Clark, S.J., Warren, M.C., Ackland, G.J., and Crain, J. (1997) Structure and elasticity of MgO at high pressure. American Mineralogist, 82, 51–60.

Kato, M. and Jordan, T.H. (1999) Seismic structure of the upper mantle beneath the western Philippine Sea. Physics of the Earth and Planetary Interiors, 110, 263–283.

Katsura, T. and Ito, E. (1989) The system Mg_2SiO_4-Fe_2SiO_4 at high pressures and temperatures: precise determination of stabilities of olivine, modified spinel, and spinel. Journal of Geophysical Research, 94, 15663–15670.

Li, B., Gwanmesia, G.D., and Liebermann, R.C. (1996) Sound velocities of olivine and beta polymorphs of Mg_2SiO_4 at Earth's transition zone pressures. Geophysical Research Letters, 23, 2259–2262.

Li, B., Liebermann, R.C., and Weidner, D.J. (1998) Elastic moduli of wadsleyite (β-Mg_2SiO_4) to 7 Gigapascals and 873 Kelvin. Science, 281, 675–677.

Mechie, J., Egorkin, A.V., Fuchs, K., Ryberg, T., Solodilov, L., and Wenzel, F. (1993) P-wave mantle velocity structure beneath northern Eurasia from long-range recordings along the profile quartz. Physics of the Earth and Planetary Interiors, 79, 269–286.

Meng, Y., Weidner, D.J., Gwanmesia, G.D., Liebermann, R.C., Vaughan, M.T., Wang, Y., Leinenweber, K., Pacalo, R.E., Yeganeh-Haeri, A., and Zhao, Y. (1993) In situ high P-T X ray diffraction studies on three polymorphs (α, β, γ) of Mg_2SiO_4. Journal of Geophysical Research, 98, 22199–22207.

Meng, Y., Fei, Y., Weidner, D.J., Dwanmesia, G.D., and Hu, J. (1994) Hydrostatic compression of γ-Mg_2SiO_4 to mantle pressures and 700 K: thermal equation of state and related thermoelastic properties. Physics and Chemistry of Minerals, 21, 407–412.

Merrill, L. and Bassett, W.A. (1974) Miniature diamond anvil pressure cell for single crystal x-ray diffraction studies. Review of Scientific Instruments, 45, 290–294.

Oreshin, S., Vinnik, L., Treussov, A., and Kind, R. (1998) Subducted lithosphere or 530 km discontinuity? Geophysical Research Letters, 25, 1091–1094.

Revenaugh, J. and Jordan, T.S. (1991) Mantle layering from ScS reverberations. 2. The transition zone. Journal of Geophysical Research, 96, 19763–19780.

Rigden, S.M., Gwanmesia, G.D., Fitz Gerald, J.D., Jackson, I., and Liebermann, R.C. (1991) Spinel elasticity and seismic structure of the transition zone of the mantle. Nature, 354, 143–145.

Rigden, S.M., Gwanmesia, G.D., Fitz Gerald, J.D., Jackson, I., and Liebermann, R.C. (1992) Progress in high-pressure ultrasonic interferometry, the pressure dependence of elasticity of Mg_2SiO_4 polymorphs and constraints on the composition of the transition zone of the Earth's mantle. In Y. Syono, and M.H. Manghnani, Eds., High-pressure research: application to Earth and planetary science, p. 167–182. Terra Publishing, Tokyo/American Geophysical Union, Washington, D.C.

Ringwood, A. (1975) Composition and petrology of the Earth's mantle. McGraw-Hill, New York.

Ryberg, T., Wenzel, F., Egorkin, A.V., and Solodilov, L. (1997) Short-period observation of the 520 km discontinuity in northern Eurasia. Journal of Geophysical Research, 102, 5413–5422.

Sawamoto, H., Weidner, D.J., Sasaki, S., and Kumazawa, M. (1984) Single-crystal elastic properties of the modified spinel (beta) phase of magnesium orthosilicate. Science, 224, 749–751.

Shearer, P.M. (1990) Seismic imaging of upper-mantle structure with new evidence for a 520-km discontinuity. Nature, 344, 121–126.

———(1991) Constraints on upper mantle discontinuities from observations of long-period reflected and converted phases. Journal of Geophysical Research, 96, 18147–18182.

———(1996) Transition zone velocity gradients and the 520-km discontinuity. Journal of Geophysical Research, 101, 3053–3066.

Sinogeikin, S.V., Bass, J.D., Kavner, A., and Jeanloz, R. (1997) Elasticity of natural majorite and ringwoodite from the Catherwood meteorite. Geophysical Research Letters, 24, 3265–3268.

Sinogeikin, S.V., Katsura, T., and Bass, J.D. (1998a) Sound velocities and elastic properties of Fe-bearing wadsleyite and ringwoodite. Journal of Geophysical Research, 103, 20819–20825.

Sinogeikin, S.V., Bass, J.D., and Katsura, T. (1998b) Elasticity of $(Mg,Fe)_2SiO_4$

spinel to transition zone pressures. EOS, Transactions American Geophysical Union, 79, F861.

Sinogeikin, S.V., Jackson, J.M., Bass, J.D., and Palko, J.W. (2000) Compact high-termperature cell for Brillouin Scattering measurements. Review of Scientific Instruments, in press.

Sumino, Y., Anderson, O.L., and Suzuki, I. (1983) Temperature coefficients of elastic constants of single-crystal MgO between 80 and 1300 K. Physics and Chemistry of Minerals, 9, 38–47.

Suzuki, I., Ohtani, E., and Kumazawa, M. (1979) Thermal expansion of γ-Mg_2SiO_4. Journal of Physics of the Earth, 27, 53–61.

Watanabe, H., (1987) Physio-chemical properties of olivine and spinel solid solutions in the system Mg_2-SiO_4-Fe_2SiO_4. In High-Pressure Research in Mineral Physics, 275–278. American Geophysical Union, Washington D.C.

Weidner, D.J. (1985) A mineral test of a pyrolite mantle. Geophysical Research Letters, 12, 417–420.

Weidner, D.J. and Carleton, H.R. (1977) Elasticity of Coesite. Journal of Geophysical Research, 82, 1334–1346.

Weidner, D.J., Sawamoto, H., Sasaki, S., and Kumazawa, M. (1984) Single-crystal elastic properties of the spinel phase of Mg_2SiO_4. Journal of Geophysical Research, 89, 7852–7860.

Whitfield, C.H., Brody, E.M., and Bassett, W.A. (1976) Elastic moduli of NaCl by Brillouin scattering at high pressure in a diamond anvil cell. Review of Scientific Instruments, 47, 942–947.

Zha, C.S., Duffy, T.S., Downs, R.T., Mao, H.K., Hemley, R.J., and Weidner, D.J. (1998) Single-crystal elasticity of the α and β of Mg_2SiO_4 polymorphs at high pressure. In M.H. Manghnani, and T. Yagi, Eds., Properties of Earth and planetary materials at high pressure and temperature, p. 9–16. American Geophysical Union, Washington, D.C.

Zouboulis, E.S. and Grimsditch, M. (1991) Refractive index and elastic properties of MgO up to 1900 K. Journal of Geophysical Research, 96, 4167–4170.